

Nucleon Electric Dipole Moments in High-Scale Supersymmetric Models

Junji Hisano^{a,b,c}, Daiki Kobayashi^b, Wataru Kuramoto^b and Takumi Kuwahara^b

^a*Kobayashi-Maskawa Institute for the Origin of Particles and the Universe (KMI),
Nagoya University, Nagoya 464-8602, Japan*

^b*Department of Physics, Nagoya University, Nagoya 464-8602, Japan*

^c*Kavli IPMU (WPI), UTIAS, University of Tokyo, Kashiwa, Chiba 277-8584, Japan*

Abstract

The electric dipole moments (EDMs) of electron and nucleons are promising probes of the new physics. In generic high-scale supersymmetric (SUSY) scenarios such as models based on mixture of the anomaly and gauge mediations, gluino has an additional contribution to the nucleon EDMs. In this paper, we studied the effect of the CP -violating gluon Weinberg operator induced by the gluino chromoelectric dipole moment in the high-scale SUSY scenarios, and we evaluated the nucleon and electron EDMs in the scenarios. We found that in the generic high-scale SUSY models, the nucleon EDMs may receive the sizable contribution from the Weinberg operator. Thus, it is important to compare the nucleon EDMs with the electron one in order to discriminate among the high-scale SUSY models.

1 Introduction

The standard model (SM) is established by the discovery of the Higgs boson with mass of 125 GeV at the LHC run 1 [1–3]. However, there are several reasons to expect that the SM must be an effective theory of a certain full theory; no candidate of the dark matter (DM), no reason of the gauge anomaly cancellation, and so on. Supersymmetry (SUSY) is one of the attractive extensions of the SM. The lightest supersymmetric particle (LSP) is the candidate of the DM. The gauge coupling unification is improved due to the additional matters, that is, the SUSY partners of the SM particles. This unification may imply that the SM gauge groups are embedded in a larger gauge group, such as $SU(5)$, $SO(10)$, and E_6 .

However, the LHC run 1 has also reported that there is no signal of new physics around electroweak (EW) scale. Besides, the observed Higgs boson is too heavy in the minimal supersymmetric standard model (MSSM) if the SUSY particle masses are smaller than $O(1)$ TeV. It is needed to introduce the large quantum correction to the Higgs mass or the additional tree-level contribution. Several extensions of the MSSM are proposed; introduction of additional vector-like matters [4], specific mass spectra (large A-term or Next-to-MSSM) [5], and high-scale SUSY scenarios [6–8].

In the high-scale SUSY scenarios, sfermions have masses around 10^2 TeV, while the gaugino masses lie around several TeV. This mass spectrum leads to the fascinating results: the SUSY flavor and CP problems are eased due to heavy sfermions [9], and the neutral wino behaves as the LSP with mass of several TeV, which is favored in the thermal DM scenario [10]. Recently, the sfermion flavor structure is focused attention on in order to survey these models by using indirect searches [11–13]. In the grand unified theories (GUTs) based on the high-scale SUSY scenarios, the specific mass spectrum yields the several features: the gauge couplings unify at the GUT scale with higher accuracy [14], and the dangerous proton decay via color-triplet Higgs exchange is suppressed due to the heavy sfermions [12, 15].

The simplest model for the high-scale SUSY scenarios is based on the anomaly mediation [16, 17]. On the other hand, the generic models may include the gauge mediated contribution to the SUSY-breaking terms [18, 19]. In the extensions, the pattern of gaugino masses differs from the simplest model. The vector-like multiplets for messengers are naturally introduced since they may obtain masses proportional to the gravitino mass via the Giudice-Masiero mechanism [20]. If we assume that the vector-like multiplets are in $SU(5)$ multiplets, the gauge coupling unification is maintained in these models. Thus, the extensions should be considered equally to the simplest model.

The electric dipole moments (EDMs) are important to investigate the additional CP violation in the SUSY breaking terms. In the SM, the EDMs for fundamental fermions are small [21], and thus the EDMs have high sensitivities on the new physics. In high-scale SUSY breaking scenarios, the generic CP -violating phases are still allowed thanks to the heavy sfermions, even if the EDMs are generated at one-loop level. However, the future experiments for EDM searches may have sensitivities to the high-scale SUSY models.

In the high-scale SUSY scenarios, the dominant contribution to the EDMs in the

MSSM comes from the Barr-Zee two-loop diagrams, especially the chargino/neutralino two-loop diagrams [22]. When the higgsino and wino are around a few TeV, the current experimental upper bound on the electron EDM has already given the constraint on the models. The ratios of electron and nucleon EDMs are predictive so that the measurements of the ratios would lead to determination of the mass spectrum.

On the other hand, there may exist additional contribution from gluino in the extended models mentioned above. The physical complex phase of the gluino mass may arise from a relative phase of the anomaly and gauge mediated contribution to it. The additional CP -violating source, so-called the gluino chromoelectric dipole moment (CEDM), is induced by the physical phase of the gluino mass and the CP -violating couplings of gluino and vector-like multiplets. The nucleon EDMs are affected by the additional source since the gluino CEDM turns into the CP -violating gluon Weinberg operator [23] below the gaugino threshold. In this paper, we study the effect of the gluino CEDM contribution to nucleon EDMs, and then we show the future prospects for the observation of EDMs (electron, neutron, and proton) in the high-scale SUSY models.

When both left- and right-handed sfermions have flavor-violating soft mass terms, the one-loop diagrams to the EDMs are enhanced by the heavy fermion masses. The contributions may be sizable when the flavor violation is $\mathcal{O}(1)$ [24–26]. However, they are quickly suppressed when the flavor violation is small. Then, we do not include the contribution to the EDMs from the flavor violation in this paper.

Current status of the EDM experiments is as follows: the bounds on the electron, neutron, and proton EDMs are given by $|d_e| < 8.7 \times 10^{-29}[e \text{ cm}]$ [27], $|d_n| < 2.9 \times 10^{-26}[e \text{ cm}]$ [28], and $|d_p| < 7.9 \times 10^{-25}[e \text{ cm}]$, respectively.¹ In future experiments, there are several proposals [30,31]: for instance, some neutron EDM measurements may achieve a sensitivity of $|d_n| \sim 10^{-28}[e \text{ cm}]$. In the proton EDM measurement at COSY [32] and BNL [33], they may achieve a sensitivity of $|d_p| \sim 10^{-29}[e \text{ cm}]$. For the electron EDM, the final purpose of the ACME experiment is to reach a sensitivity of $3 \times 10^{-31}[e \text{ cm}]$. If the electron and nucleon EDMs are discovered, we may discriminate models beyond the SM by taking correlation among them.²

This paper is organized as follows: in Section 2, we introduce the high-scale SUSY scenarios with the gauge mediation and show that the physical phase of the gaugino mass appears. The complex gluino mass gives rise to the gluino CEDM, and the CP -violating Weinberg operator [23] is induced by integrating out the gluino field in the scenarios. The gluino CEDM and the Weinberg operator in the scenarios are shown in Section 3. In the next section, we briefly introduce our method to estimate the observable EDMs, in particular neutron and proton EDMs. The contributions of (C)EDMs of quarks to the nucleon EDMs are evaluated with the QCD sum rules, while those of the Weinberg operator are based on the naive dimensional analysis. We give the detail of calculations in Appendices A and B. In Section 5, we study the effect of gluino CEDM to nucleon EDMs. We evaluate the electron, proton, and neutron EDMs in the high-scale SUSY scenarios in the last of this section. Finally, we summarize this paper in Section 6.

¹ The proton EDM is deduced from the Mercury EDM [29].

² See Ref. [34] and the references in it for the recent works.

2 Complex Gaugino Mass

In the SUSY breaking sector, we assume that there is no singlet superfield. Under this assumption, the soft parameters are given as follows: mass parameters of scalar components are induced by the Planck-suppressed higher-dimensional operators, and gaugino masses and scalar trilinear couplings are induced with one-loop suppression by the anomaly mediation [16,17]. In particular, the anomaly mediated gaugino masses are given by

$$M_a^{\text{AMSB}} = \frac{\beta(g_a)}{g_a} m_{3/2}, \quad (1)$$

where the subscripts $a = 1-3$ denote the gauge groups of the SM, $U(1)_Y$, $SU(2)_L$, and $SU(3)_C$. $\beta(g_a)$ and $m_{3/2}$ denote the beta function for the gauge coupling g_a and the gravitino mass, respectively.

We note that there also exists the additional contribution from the higgsino-Higgs loops to the wino and bino masses. Below the higgsino threshold, the additional contribution is given as [16]

$$M_1^{\tilde{h}H} = \frac{g_1^2}{16\pi^2} \frac{3}{5} L, \quad M_2^{\tilde{h}H} = \frac{g_2^2}{16\pi^2} L. \quad (2)$$

The parameter L denotes the loop function defined as

$$L = \mu_H \sin 2\beta \frac{m_A^2}{|\mu_H|^2 - m_A^2} \ln \frac{|\mu_H|^2}{m_A^2}, \quad (3)$$

where μ_H and m_A denote the masses of higgsino and heavy Higgs bosons, respectively. $\tan \beta$ denotes the ratio of the vacuum expectation values (VEVs) of MSSM Higgs bosons.

If there exist vector-like superfields, so-called messenger multiplets of the gauge mediation, the soft parameters differ from the simple high-scale SUSY breaking scenario. In order to maintain the gauge coupling unification, we assume that messenger superfields are in $\mathbf{5} + \overline{\mathbf{5}}$ or $\mathbf{10} + \overline{\mathbf{10}}$ representation. The mass terms of the messenger superfields arise from the Giudice-Masiero mechanism [20], if the Kähler potential is given as

$$\mathcal{K} = |\overline{\Phi}|^2 + |\Phi|^2 + (c_\Phi \overline{\Phi} \Phi + \text{h.c.}), \quad (4)$$

where Φ and $\overline{\Phi}$ denote the messenger chiral superfields. On the other hand, the superpotential $W(\Phi, \overline{\Phi})$ may have the mass terms of the messenger superfields,

$$W(\Phi, \overline{\Phi}) = M_\Phi \overline{\Phi} \Phi. \quad (5)$$

In those cases, the mass matrix of the scalar components of Φ and $\overline{\Phi}$ is given as

$$\mathbf{m}_\phi^2 = \begin{pmatrix} |M_\Phi + c_\Phi m_{3/2}|^2 & c_\Phi^* m_{3/2}^2 \\ c_\Phi m_{3/2}^2 & |M_\Phi + c_\Phi m_{3/2}|^2 \end{pmatrix} \equiv \begin{pmatrix} |M|^2 & -|F|e^{-i\theta_F} \\ -|F|e^{i\theta_F} & |M|^2 \end{pmatrix}, \quad (6)$$

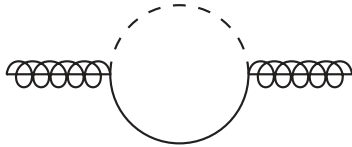


Figure 1: One-loop diagram contributing to gluino mass. Solid and dashed lines correspond to the propagators of fermionic and scalar components of chiral multiplets $\Phi, \bar{\Phi}$, respectively.

where the term proportional to $m_{3/2}$ arises from the Giudice-Masiero mechanism. For simplicity, the mass parameters are re-parametrized by M and F in the last form, and θ_F denotes the complex phase of F .

In the above models, the gaugino masses are induced by the anomaly and gauge mediation mechanisms at one-loop order. The anomaly mediated gluino mass is given by [16, 17]:

$$M_3^{\text{AMSB}} = \frac{g_3^2}{16\pi^2} b_3 m_{3/2} . \quad (7)$$

$b_3 = -3 + N_{\mathbf{5}} + 3N_{\mathbf{10}}$ is the coefficient for the one-loop beta function of the $SU(3)_C$ gauge coupling, where $N_{\mathbf{5}}$ and $N_{\mathbf{10}}$ denote the numbers of pairs of $\mathbf{5} + \bar{\mathbf{5}}$ and $\mathbf{10} + \bar{\mathbf{10}}$ representations, respectively. We choose M_3^{AMSB} as real for simplicity. M_3^{GMSB} is induced by a diagram in Fig. 1 [35]:

$$M_3^{\text{GMSB}} = \frac{g_3^2}{16\pi^2} (\cos \theta_F - i \sin \theta_F \gamma_5) n_3(\Phi) \left| \frac{F}{M} \right| g(x) , \quad (8)$$

where $x \equiv |F/M^2|$ and $n_3(\Phi)$ is the sum of Dynkin indices of the pair of chiral multiplets, Φ and $\bar{\Phi}$. The loop function $g(x)$ is given by

$$g(x) = \frac{(1+x) \ln(1+x) + (1-x) \ln(1-x)}{x^2} . \quad (9)$$

For later use, we define the real gluino mass parameter $M_{\tilde{g}}$ and the phase of the gluino mass θ as:

$$M_{\tilde{g}} e^{i\gamma_5 \theta} = M_3^{\text{AMSB}} + M_3^{\text{GMSB}} . \quad (10)$$

By the chiral rotation of the gluino field $\tilde{g}^a \rightarrow \tilde{g}'^a = e^{-i\theta\gamma_5/2} \tilde{g}^a$, this additional complex phase appears in the interaction terms between gluino and messengers. In next section, we show that the additional complex phase gives rise to the gluino CEDM, and then the CP -violating Weinberg operator also arises from the gluino CEDM operator below the gluino threshold scale.

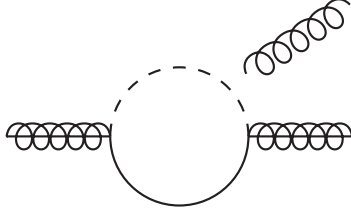


Figure 2: One-loop diagram inducing gluino CEDM. Solid and dashed lines correspond to propagators of fermionic and scalar components of chiral multiplets $\Phi, \bar{\Phi}$, respectively.

3 Gluino CEDM and Weinberg Operator

In our models, the gluino CEDM is generated by the messenger loop diagrams (Fig. 2) since there exists the non-vanishing CP -violating phase in the gluino-messenger interaction after the chiral rotation of the gluino. The gluino CEDM $d_{\tilde{g}}$ is given as

$$\mathcal{L}_{\tilde{g} \text{ CEDM}} = -\frac{i}{4} \tilde{d}_{\tilde{g}} \bar{\tilde{g}}^b \sigma^{\mu\nu} \gamma_5 G_{\mu\nu}^a [T^a]_{bc} \tilde{g}^c, \quad (11)$$

where $\sigma^{\mu\nu} = \frac{i}{2}[\gamma^\mu, \gamma^\nu]$ and $G_{\mu\nu}^a = \partial_\mu G_\nu^a - \partial_\nu G_\mu^a + g_3 f^{abc} G_\mu^b G_\nu^c$. $[T^a]_{bc} = -if^{abc}$ and f^{abc} is the structure constant for the $SU(3)_C$.

We estimate the relevant CP -violating terms at the gluino mass scale ($M_{\tilde{g}}$) from those at the messenger mass scale (M_{mess}) by using the renormalization group equation (RGE) analysis. It is useful to define the dimension-six gluino CEDM operator in order to estimate the RGE evolution. The gluino CEDM operator $\mathcal{O}_{\tilde{g}}$ and its Wilson coefficient $C_{\tilde{g}}$ are defined as

$$\mathcal{O}_{\tilde{g}} = \frac{1}{4} M_{\tilde{g}} g_3 f^{abc} \bar{\tilde{g}}^a \sigma^{\mu\nu} \gamma_5 \tilde{g}^c G_{\mu\nu}^b, \quad \tilde{d}_{\tilde{g}} = M_{\tilde{g}} g_3 C_{\tilde{g}}. \quad (12)$$

By evaluating a diagram in Fig. 2, we obtain the Wilson coefficient of $\mathcal{O}_{\tilde{g}}$ as

$$C_{\tilde{g}}(M_{\text{mess}}) = -\frac{g_3^2}{32\pi^2} \frac{1}{M_{\tilde{g}}} \frac{M}{m_+^2} \sin(\theta + \theta_F) [A(r_+) + B(r_+)] - (m_+, r_+ \rightarrow m_-, r_-), \quad (13)$$

where $m_\pm^2 = |M|^2 \pm |F|$ are the mass eigenvalues of the mass matrix for the scalar components of Φ and $\bar{\Phi}$, and $r_\pm = |M|^2/m_\pm^2$. θ and θ_F are respectively the phases of the complex gluino mass and the off-diagonal element F of the mass matrix \mathbf{m}_ϕ^2 , as defined in the previous section. The loop functions $A(r)$ and $B(r)$ are given as

$$A(r) \equiv \frac{1}{2(1-r)^2} \left(3 - r + \frac{2 \ln r}{1-r} \right), \quad B(r) \equiv \frac{1}{2(1-r)^2} \left(1 + r + \frac{2r \ln r}{1-r} \right). \quad (14)$$

Now, we estimate the gluino CEDM at the gluino mass scale by using the RGEs between the messenger and the gluino mass scales. The RGE for the Wilson coefficient

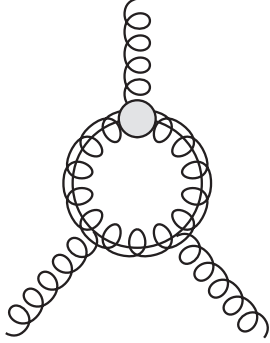


Figure 3: One-loop diagram inducing CP -violating Weinberg operator. The blob denotes the gluino CEDM operator.

$C_{\tilde{g}}(\mu)$ at the leading order is given as

$$\frac{\partial}{\partial \ln \mu} C_{\tilde{g}}(\mu) = \frac{g_3^2}{16\pi^2} \gamma_{\mathcal{O}_{\tilde{g}}} C_{\tilde{g}}(\mu) , \quad (15)$$

where $\gamma_{\mathcal{O}_{\tilde{g}}} = 12N_C$ and $N_C (= 3)$ is the number of colors. This anomalous dimension is found by substituting the Casimir invariant $C_F = N_C$ for $C_F = 4/3$ in the anomalous dimension of the dipole operator for $b \rightarrow sg$ [36, 37]. The gluino CEDM at the gluino mass scale is obtained as follows:

$$\frac{\tilde{d}_{\tilde{g}}(M_{\text{mess}})}{\tilde{d}_{\tilde{g}}(M_{\tilde{g}})} = \left(\frac{\alpha_s(M_{\text{mess}})}{\alpha_s(M_{\tilde{g}})} \right)^{\gamma_{\mathcal{O}_{\tilde{g}}}/2b_3 - 3N_C/b_3 + 1/2} . \quad (16)$$

Here, $b_3 = -7|_{\text{SM}} + 2|_{\text{gluino}}$ where the subscripts ‘‘SM’’ and ‘‘gluino’’ indicate the contribution from the SM particles and gluino, respectively. The exponents $-3N_C/b_3$ and $1/2$ are due to the one-loop renormalization-group evolution of the gluino mass $M_{\tilde{g}}$ and the strong gauge coupling g_3 , respectively.

The CP -violating Weinberg operator is induced through the gluino one-loop diagram in Fig. 3. The effective Lagrangian for the Weinberg operator is defined as [23]

$$\mathcal{L}_W = C_W \mathcal{O}_W, \quad \mathcal{O}_W = -\frac{1}{6} g_3 f^{abc} \epsilon^{\mu\nu\rho\sigma} G_{\mu\lambda}^a G_{\nu}^{b\lambda} G_{\rho\sigma}^c . \quad (17)$$

Here, $\epsilon^{\mu\nu\rho\sigma}$ is the totally-antisymmetric tensor with $\epsilon^{0123} = +1$. At the gluino mass scale, we obtain the Wilson coefficient of the Weinberg operator by matching the amplitude as follows³:

$$C_W(M_{\tilde{g}}) = \frac{N_C g_3^2}{32\pi^2} C_{\tilde{g}}(M_{\tilde{g}}) . \quad (18)$$

³ In Refs [38–41], authors considered the similar effects arising from the CP -violating coupling of heavy quarks.

Notice that quark (C)EDMs are induced as a three-loop contribution after integrating out the messenger multiplets. The Weinberg operator could be also induced directly after squarks and messenger multiplets are integrated out, not via the gluino CEDM. These contributions are suppressed by the masses of squarks and messenger multiplets. Thus, the gluino CEDM contribution is dominant for the Weinberg operator as far as gluino is lighter than them.

4 Nucleon Electric Dipole Moments

In previous section, we show the expression of the CP -violating Weinberg operator induced by the gluino CEDM at the gluino mass scale. The quark EDMs are also induced through the Barr-Zee diagrams [42], which are dominated by only the chargino and neutralino loops in the MSSM based on the high-scale SUSY scenarios [22]. The quark CEDMs are radiatively induced from the Weinberg operator so that they are subdominant.

In this section, we summarize the RGE evolutions of the CP -violating operators and results of the QCD sum rules and the naive dimensional analysis in order to obtain the nucleon EDMs at the hadron scale ($\mu = 1 \text{ GeV}$) in a compressed way.

The CP -violating operators in the QCD sector below the gluino mass scale are given as

$$\begin{aligned} \mathcal{L}_{\mathcal{CP}} = & \bar{\theta} \frac{g_3^2}{32\pi^2} G_{\mu\nu}^a \tilde{G}^{a,\mu\nu} \\ & - \frac{i}{2} \sum_{q=u,d,s} d_q \bar{q} (F \cdot \sigma) \gamma_5 q - \frac{i}{2} \sum_{q=u,d,s} \tilde{d}_q g_3 \bar{q} (G \cdot \sigma) \gamma_5 q \\ & + \frac{1}{3} w f^{abc} G_{\mu\nu}^a \tilde{G}^{b,\nu\rho} G_{\rho\mu}^c . \end{aligned} \quad (19)$$

Here, $F_{\mu\nu}$ and $G_{\mu\nu}^a$ are the electromagnetic and gluon field strength tensors, respectively, and we define as $F \cdot \sigma = F_{\mu\nu} \sigma^{\mu\nu}$ and $G \cdot \sigma = G_{\mu\nu}^a \sigma^{\mu\nu} T^a$. The dual field strength tensor is defined as $\tilde{G}^{a,\mu\nu} = \frac{1}{2} \epsilon^{\mu\nu\rho\sigma} G_{\rho\sigma}^a$. The first term of Eq. (19) is the dimension-four CP -violating term, so-called QCD θ -term. Since this operator, however, does not mix with the other operators, we neglect the QCD θ -term in the RGE analysis. The second and third terms of Eq. (19) correspond to the quark EDMs and CEDMs, respectively. The last term is the Weinberg operator [23]. The coefficient of the Weinberg operator w is given as $w = -g_3 C_W$, which is evaluated in the previous section.

In our numerical evaluation of the nucleon EDMs, we include the RGE evolutions of these operators between the gluino mass scale and the scale of $\mu = 1 \text{ GeV}$. The RGEs for the Wilson coefficients at the leading order are given by Ref. [37]. The detail of RGEs with mixing of the quark (C)EDMs and the CP -violating Weinberg operator is given in Appendix A.

Next, we show the nucleon EDMs induced by the quark (C)EDMs via the QCD sum rules. In Ref. [43], the neutron EDM d_n is related to the quark (C)EDMs by using the

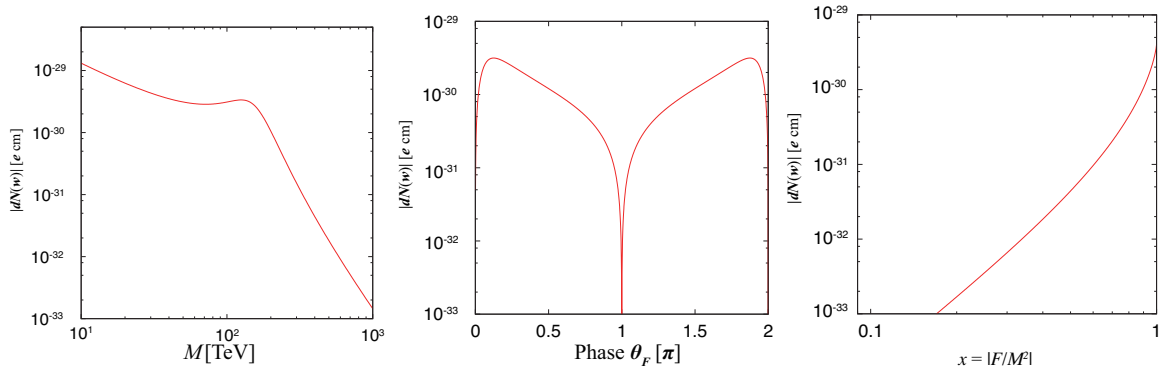


Figure 4: Parameter dependence of $d_N(w)$ with fixed sfermion mass scale ($M_S = 100$ TeV). (Left): Messenger mass M dependence with $\theta_F = 0.125\pi$ and $x = 0.99$. (Middle): Phase θ_F dependence with $M = M_S$ and $x = 0.99$. (Right): x ($\equiv |F/M^2|$) dependence with $\theta_F = 0.125\pi$ and $M = M_S$.

QCD sum rules at the renormalization scale $\mu = 1$ GeV. Similarly, the proton EDM d_p is also associated with the quark (C)EDMs at the scale of $\mu = 1$ GeV. We obtain the relation between the EDMs for light nucleons and the quark (C)EDMs as follows:

$$\begin{aligned} d_p &= -1.2 \times 10^{-16} [e \text{ cm}] \bar{\theta} + 0.78d_u - 0.20d_d + e(-0.28\tilde{d}_u + 0.28\tilde{d}_d + 0.021\tilde{d}_s), \\ d_n &= 8.2 \times 10^{-17} [e \text{ cm}] \bar{\theta} - 0.12d_u + 0.78d_d + e(-0.30\tilde{d}_u + 0.30\tilde{d}_d - 0.014\tilde{d}_s). \end{aligned} \quad (20)$$

The explicit formulae and the numerical values are presented in Appendix B. The quark EDM contributions to the neutron EDM are consistent with the recent result with the lattice QCD simulation [44]. In the following numerical analyses, we use the results from the QCD sum rules with $\bar{\theta} = 0^4$.

The nucleon EDMs induced by the Weinberg operator are given by [45]:

$$d_N(w) \sim e(10 - 30) \text{ MeV } w(1 \text{ GeV}), \quad (N = n, p). \quad (21)$$

This is based on the naive dimensional analysis. The sign of the contribution of the Weinberg operator is also ambiguous. We adopt the value $d_N(w)/e = 20 \text{ MeV } w(1 \text{ GeV})$ as the nucleon EDMs induced by Weinberg operator in the following numerical analyses.

5 Numerical Results

Now, we estimate the electron and nucleon EDMs in the high-scale SUSY scenarios.

⁴ If we impose the Peccei-Quinn symmetry, the theta parameter $\bar{\theta}$ is induced, and the formulae for the nucleon EDMs are changed (the explicit expressions are given in the Appendix B), especially the coefficients of \tilde{d}_q . However, in our study, the quark CEDMs are subdominant since they are induced only through the RGEs, and our results are almost unchanged in each case.

To begin with, let us consider the parameter dependence of nucleon EDMs induced by the gluino CEDM. In this evaluation, we assume that sfermions, heavy Higgs bosons and the gravitino are degenerate in mass M_S , and we take $M_S = 100$ TeV. Once we fix M_S , we have three parameters; M and $|F|$ which are the mass parameters of the scalar fields of messengers, and θ_F which is the complex phase of F . In the following numerical analyses, we choose M , θ_F , and $x (\equiv |F/M^2|)$ as independent parameters.

Fig. 4 shows parameter dependence of the nucleon EDMs d_N ($N = p, n$) induced by the gluino CEDM. In the middle panel of Fig. 4, we show the θ_F dependence of gluino-induced nucleon EDMs. In this figure, we set $M = 100$ TeV and $x = 0.99$. If $\theta_F = 0$ or π , there is no contribution from the gluino-induced nucleon EDM, since M^{GMSB} and the couplings of the gluino-messenger interaction are real. The maximal contribution is given by $\theta_F \sim 0.125\pi$. When the real and imaginary parts of the gluino mass are comparable to each other, the physical phase of the gluino mass θ is maximized. Since the coefficient of the Weinberg operator is proportional to $\sin(\theta + \theta_F)/M_{\tilde{g}}$, the maximum contribution arises when $\theta + \theta_F \sim \pi/2$ and $M_{\tilde{g}}$ is small.

In the right of Fig. 4, the x dependence of nucleon EDM is shown. This dependence is evaluated with $M = 100$ TeV and $\theta_F = 0.125\pi$. The gluino CEDM approaches to the maximum as $x \rightarrow 1$. On the other hand, one of the scalars of messengers becomes massless when $x = 1$. In order to avoid this situation, in the following calculations, we set $x = 0.99$ for simplicity.

Finally, we show the M dependence of nucleon EDM in the left panel of Fig. 4. In this figure, we set $x = 0.99$ and $\theta_F = 0.125\pi$. The Wilson coefficient of Weinberg operator (Eq. (18)) behaves as follows:

$$C_W \propto \begin{cases} \frac{1}{M_S M} \sin(\theta + \theta_F) & (M \ll M_S), \\ \frac{1}{M^2} \sin(\theta + \theta_F) & (M_S \ll M). \end{cases} \quad (22)$$

When $M \gg M_S$, the gluino mass mainly comes from the gauge mediation so that the Weinberg operator is highly suppressed by M^2 and also the suppressed CP phase in $\sin(\theta + \theta_F)$. If $M \ll M_S$, the gluino mass is dominated by the anomaly mediated contribution, and thus, the Weinberg operator is suppressed by $M_S M$. On the other hand, in the region $M \sim M_S$, the nucleon EDMs are slightly enhanced since the gauge mediated gluino mass is comparable to M^{AMSB} and thus the CP phase of the gluino mass is maximal.

Now, let us compare the nucleon and electron EDMs in the high-scale SUSY scenarios, in which the Barr-Zee diagrams and gluino CEDM contribute to the EDMs. In the high-scale SUSY scenarios, all MSSM scalar particles except the SM Higgs multiplet are assumed to be heavy. Within the MSSM, the main contributions to the electron and nucleon EDMs arise from the Barr-Zee type two-loop diagram contributions [22]. The diagrams include loops of charginos and neutralinos, and the contributions to EDMs are suppressed by $m_f/M_2\mu_H^5$. (The electron or quark mass m_f appears in the quark and

⁵ This behavior of the Barr-Zee contribution is understood by using the effective theory of wino after integrating out higgsino [46].

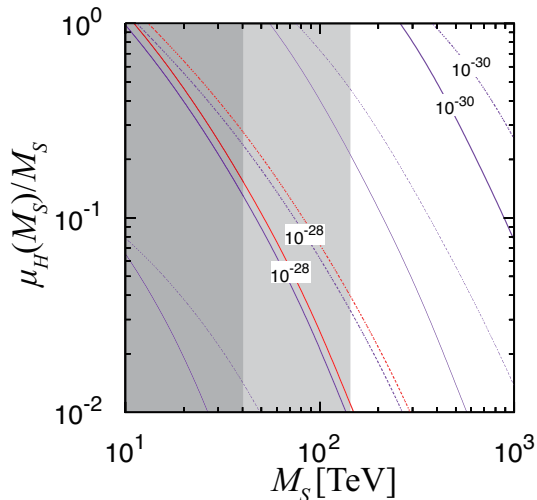


Figure 5: Electron EDM in high-scale SUSY models with $N_{\mathfrak{F}} = 0$ (dotted) and 1 (solid). Red lines correspond to the current bound; $|d_e| < 8.7 \times 10^{-29} [e \text{ cm}]$ [27]. Dark gray and light gray regions are excluded by gluino search at the LHC with $N_{\mathfrak{F}} = 0$ and 1, respectively.

electron EDMs due to the chiral nature.) Since the higgsino mass μ_H is a model-dependent parameter, we perform the evaluation of EDMs in a range of $\mu_H/M_S \in [10^{-2}, 1]$. The CP phase of μ_H is also model-dependent and therefore we set the CP phase in the mass matrices of charginos and neutralinos to make the Barr-Zee contributions maximized⁶. We note that we set $\tan\beta = 3$ since $\tan\beta$ is also model-dependent parameter⁷.

In the following numerical analyses, we assume that all MSSM scalar particles except the SM Higgs boson have the same mass M_S and three parameters which are associated with the gluino induced nucleon EDMs are set to be $M = M_S$, $\theta_F = 0.125\pi$, and $x = 0.99$ in order to study the maximal gluino CEDM effects. The higgsino mass μ_H is estimated as follows: input value for the higgsino mass is given at the renormalization scale $\mu = M_S$, and then, we estimate the higgsino mass at $\mu = \mu_H(M_S)$ by using the one-loop RGEs for higgsino and gauginos.

The Barr-Zee contributions are estimated as follows: the input parameters for the chargino and neutralino mass matrices are estimated at $\mu = \mu_H(M_S)$, the coupling

⁶ In the Ref. [22], there exist two independent phases ϕ_1 and ϕ_2 , which are the combinations of phases of gaugino masses, gaugino-higgsino-Higgs couplings, and μ_H . We set $\sin\phi_1 = \sin\phi_2 = 1$ in our numerical analyses, unless otherwise stated. However, since there remain the two ambiguities to determine the nucleon EDMs. One is the sign ambiguity in the contribution of the Weinberg operator to the nucleon EDMs. The other is the choice of the independent phases as $\sin\phi_1 = \sin\phi_2 = -1$, which is also allowed to maximize the absolute value of the Barr-Zee contribution. There is no need to care about these ambiguities as far as discussing absolute values for each contributions.

⁷We do not take care of whether the observed Higgs mass is realized in the parameter set in this paper, though we set the Higgs mass in the Barr-Zee contributions to be the observed value. If there exist additional matters contributing to the Higgs mass (such as Ref. [47]), the favored values for $\tan\beta$ to realize the observed Higgs mass may differ from those in the simple high-scale SUSY models [6, 7].

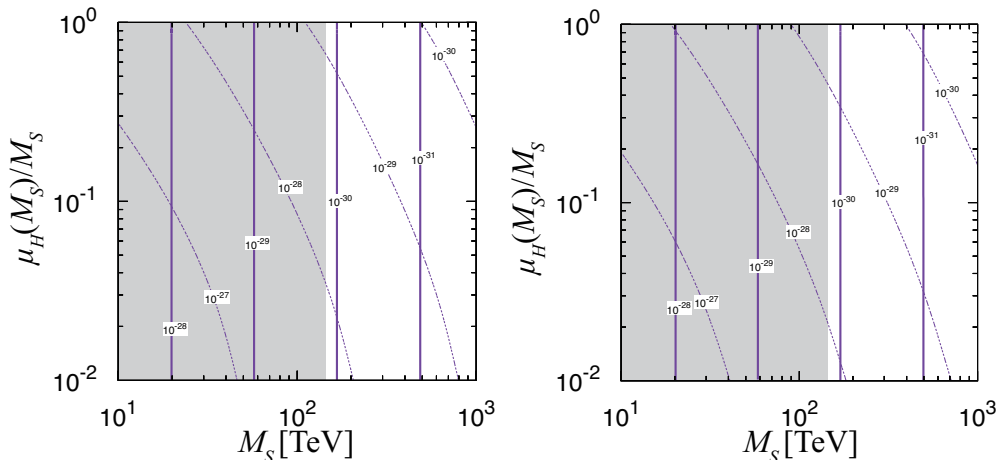


Figure 6: Nucleon EDMs from Barr-Zee diagrams and gluino CEDM. Neutron (proton) EDM is shown in left (right) panel. Dotted lines describe the case of vanishing gluino CEDM, that is, we set $\theta_F = 0$. Solid lines correspond to the case of vanishing Barr-Zee contribution. Again, gray regions in each figures are excluded by gluino search at the LHC. In each panels, number of messengers is set to be $N_{\mathfrak{F}} = 1$.

constants associated with the chargino and neutralino loops are also estimated at $\mu = \mu_H(M_S)$, and other couplings are estimated at the EW scale.

First, we show electron EDM d_e in the high-scale SUSY scenarios (Fig. 5). We assume that there is no messenger superfield ($N_{\mathfrak{F}} = 0$; dotted lines in Fig. 5) and that there is messenger superfields ($N_{\mathfrak{F}} = 1$; solid lines in Fig. 5). The dark (light) shaded regions are excluded by the gluino search at the LHC [48, 49], that is, $M_g^{\text{pole}} < 1.3$ TeV. The red lines correspond to the current bound on the electron EDM measured by the ACME experiment, $|d_e| < 8.7 \times 10^{-28} e$ cm. It is found that the future experiment for the electron EDM may have sensitivities to the SUSY breaking scale of $M_S \sim 10^3$ TeV in each scenario.

In the high-scale SUSY models with messengers, there are several differences from the models with no messengers. One is that the constraint on the SUSY breaking scale becomes severe in the models with messengers. This is because that the cancellation between the anomaly and gauge mediated contributions reduce the gluino mass since we choose parameters to maximize the gluino CEDM. Another is that the Barr-Zee contributions are slightly suppressed since the masses of wino and bino become large in the extended models.

Next we investigate the nucleon EDMs in the high-scale SUSY models. First, we compare the nucleon EDMs induced by only the gluino CEDM with the Barr-Zee contribution. In Fig. 6, we show the nucleon EDMs induced by only the gluino CEDM (solid lines) or the Barr-Zee contribution (dotted lines). The neutron (proton) EDM is shown in the left (right) panel of Fig. 6. If the Barr-Zee contributions vanish, the nucleon EDMs are induced by only the gluino CEDM. The nucleon EDMs induced by only the gluino CEDM are almost the same even if the quark (C)EDMs are induced via the RG mixing.

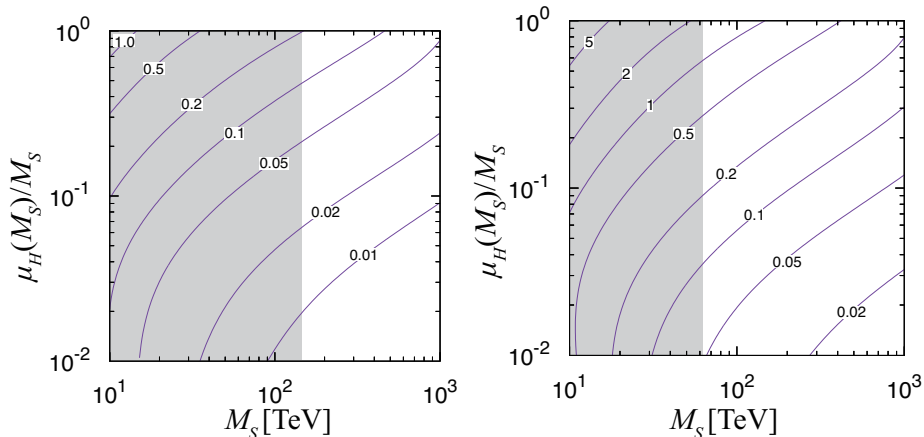


Figure 7: Ratio of d_{nW}/d_{nBZ} with mass of messengers to be M_S ($0.1M_S$) in left (right) figure. Shades in each figures show excluded region by gluino search at the LHC, again. In each figures, we set number of messengers to be $N_{\mathfrak{S}} = 1$.

On the other hand, if there is no physical phase of the gluino mass, the nucleon EDMs come from the Barr-Zee contributions. The Barr-Zee contributions are suppressed in the region of heavy higgsino and gauginos. Since there remains the ambiguity in the relative sign between the Barr-Zee contribution and the Weinberg operator, the nucleon EDMs are not determined if there exist both contributions. However, it is found that these contributions may be comparable in some region, especially heavy higgsino. Thus, we need to include the gluino CEDM contribution to determine precisely the nucleon EDMs.

Now, let us estimate the ratio of neutron EDMs induced by the Barr-Zee diagrams and the Weinberg operator. In this evaluation, we fix the phases of Barr-Zee contributions as mentioned above, and we also estimate the quark (C)EDMs and the Weinberg operator at 1 GeV with the RGEs. In Fig. 7, we show the ratios of the neutron EDMs induced by the Weinberg operator (d_{nW}) and induced by the Barr-Zee diagrams (d_{nBZ}). Since the quark (C)EDMs and the Weinberg operator mix with each other, it is not obvious to discriminate between the neutron EDM derived from quark (C)EDMs and that derived from the Weinberg operator at low energy. We, however, identify the neutron EDM induced by the Barr-Zee contribution (d_{nBZ}) with d_n defined in Eq. (20), which is dominated by the Barr-Zee contribution since the RGE effect is negligible due to the one-loop suppression. Similarly, one induced by the Weinberg operator (d_{nW}) is identified with $d_n(w)$ defined in Eq. (21).

In the left figure of Fig. 7, we show the ratio $|d_{nW}/d_{nBZ}|$, taking the messenger mass to be M_S . (We will discuss the right figure of Fig. 7 below.) In the large μ_H limit, the Barr-Zee contributions are suppressed since the EDMs induced by the Barr-Zee diagrams proportional to $d_f \sim m_f/M_2\mu_H$ as mentioned above. On the other hand, in the small M_S region, the neutron EDM induced by the gluino CEDM is enhanced due to the smallness of the gluino mass. Thus, in the region of small M_S and large higgsino mass, the dominant contribution arises from gluino CEDM, though such a region is constrained by the gluino

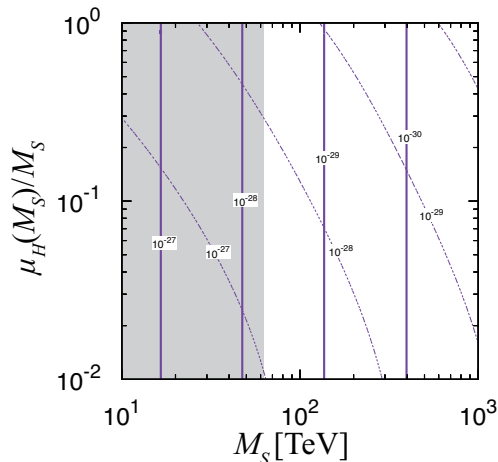


Figure 8: Neutron EDMs from the Barr-Zee diagrams and the gluino CEDM in the light messenger case ($M = 0.1M_S$). Dotted lines describe the case of no gluino CEDM. Solid lines correspond to the case of no Barr-Zee contribution. The gray regions in each figures are excluded by the gluino search at the LHC. The number of messengers is set to be $N_{\mathfrak{S}} = 1$.

search at the LHC.

In the last of this section, let us consider the case of light messengers. The light messengers would realized if some symmetry is imposed to the messengers. As mentioned in the beginning of this section, the gluino CEDM is induced by the CP -violating coupling of gluino and messengers since the gluino mass is dominated by the anomaly mediated one. If the messengers have the mass lighter than M_S , the suppression of the gluino CEDM becomes mild. Therefore, the nucleon EDMs induced by the gluino CEDM become large in comparison with the heavy messenger case.

In the light messenger case, since the gaugino masses are dominated by the anomaly mediated contribution, the phase of the gluino mass θ in the case is approximately zero, and then the gluino CEDM is proportional to $\sin \theta_F$. Thus, in the following numerical evaluation, we set $\theta_F = \pi/2$ in order to maximize the gluino CEDM. If the supersymmetric masses of messengers are sufficiently light, the lightest scalars of messengers may have masses much lighter than the EW scale. In the following analysis, the scale of messengers is set to be $M = 0.1M_S$ in order to avoid too light scalars of messengers while x is 0.99.

We show the neutron EDM in the light messenger case in Fig. 8. The dotted and solid lines respectively describe the cases of no gluino CEDM and no Barr-Zee contribution. In this case, the neutron EDM via the gluino CEDM become larger than in the case of heavy messengers, as expected. On the other hand, the Barr-Zee contributions are the same in size as the case of heavy messengers. Therefore, the gluino CEDM gives the sizable contribution to the neutron EDM. If there exist both of the Barr-Zee and gluino CEDM contributions, the nucleon EDMs may be enhanced or suppressed. However, we do not evaluate the nucleon EDMs in this case since we have the sign ambiguity for the

Weinberg operator in the nucleon EDMs.

As is the case for the heavy messenger, we also show the ratio of each contribution with light messengers (in the right figure of Fig. 7). In this case ($M < M_S$), the contribution from the Weinberg operator is enhanced due to the light messenger mass as mentioned in Eq. (22). Thus, the d_{nW} dominates the neutron EDMs in a broad region in the light messenger scenario.

In Fig. 6, we have shown that the proton EDMs induced by the Barr-Zee diagrams and the gluino CEDM behave similar as the neutron EDMs. The behavior of the proton EDM is also similar to the neutron EDM in the light messenger scenario. Since the future experiments of the proton EDM may have sensitivities to $|d_p| \sim 10^{-29} e \text{ cm}$, the gluino CEDM effect via the proton EDM may be found.

Before we conclude this paper, we mention the uncertainty of numerical calculation. The error of $\alpha_s(M_Z) = 0.1185 \pm 0.0006$ gives uncertainty on the results about $\mathcal{O}(1)\%$ and then it does not appear in the numerical analyses. Thus, the uncertainties mainly come from the QCD sum rules and the naive dimensional analysis which we use in order to obtain the nucleon EDMs from the quark (C)EDMs and the Weinberg operator. Especially, the uncertainty in the naive dimensional analysis should be large so that we might expect larger contributions from the gluino CEDM to the nucleon EDMs. Furthermore, in the above, we assume $N_{\mathbf{5}} = 1$ and $N_{\mathbf{10}} = 0$ for simplicity. If more messenger fields are introduced, larger contribution from the gluino CEDM to the nucleon EDMs is expected if the CP phases are aligned to be constructive.

6 Conclusion and Discussion

In this paper, we estimated the nucleon and electron EDMs in the high-scale SUSY models. Even if the gaugino masses induced by the anomaly mediation are real, the additional contributions to gaugino masses may give rise to the physical phases of gaugino masses. We show the case in the high-scale SUSY models which is based on the mixture of anomaly and gauge mediations. In particular, the gluino CEDM is induced by the physical phase of the gluino mass mass and the CP -violating couplings of gluino, and then it generates the CP -violating Weinberg operator.

We estimated the effect of the gluino CEDM in the extension of high-scale SUSY scenarios, and we showed the nucleon EDMs induced by the gluino CEDM and the Barr-Zee contributions. The dominant contribution to the nucleon EDMs within the MSSM comes from the Barr-Zee contribution of chargino/neutralino loops at two-loop level, while one-loop diagrams of the messenger particles generate the gluino CEDM. We revealed that the gluino CEDM may affect on the prediction of EDMs of nucleons in the high-scale SUSY models, especially in the cases of the light messengers or heavy higgsino in comparison with M_S . We do not determine the total EDMs for nucleons since we still have large ambiguities in the naive dimensional analysis for the Weinberg operator, including the sign. If it is determined precisely, the proton and neutron EDMs may be found to behave differently in the extended models, and thus, it would be more important to detect

nucleon EDMs and electron EDM or the ratios of them.

Acknowledgments

We thank Dr. Natsumi Nagata for useful discussion. This work is supported by Grant-in-Aid for Scientific research from the Ministry of Education, Science, Sports, and Culture (MEXT), Japan, No. 23104011 (J.H.). The work of J.H. is also supported by World Premier International Research Center Initiative (WPI Initiative), MEXT, Japan. The work of D.K. is supported by Grant-in-Aid for Japan Society for the Promotion of Science (JSPS) Fellows (No. 26004521).

Appendix

A Renormalization Group Equations

The (flavor-diagonal) CP -violating operators below the electroweak scale are given up to dimension-six operators as defined in Eq. (19). For considering the RGE evolutions of these operators, it is convenient to define the quark (C)EDM operators \mathcal{O}_i^q ($i = 1, 2$) as

$$\mathcal{O}_1^q = -\frac{i}{2}m_q e e_q \bar{q}(F \cdot \sigma)\gamma_5 q, \quad \mathcal{O}_2^q = -\frac{i}{2}m_q \bar{q}g_3(G \cdot \sigma)\gamma_5 q. \quad (23)$$

e_q denotes the electric charge of the quark q and g_3 is the QCD coupling constant. The Weinberg operator is also given by \mathcal{O}_W as in Eq. (17). Then, by using these operators, the effective Lagrangian is rewritten as follows:

$$\mathcal{L}_{\mathcal{CP}} = \sum_{i=1}^2 \sum_{q=u,d,s} C_i^q \mathcal{O}_i^q + C_W \mathcal{O}_W. \quad (24)$$

The relation between the coefficients in the Lagrangian in Eq. (19) and the Wilson coefficients is given by:

$$d_q = m_q e e_q C_1^q, \quad \tilde{d}_q = m_q C_2^q, \quad w = -g_3 C_W. \quad (25)$$

The RGEs for the Wilson coefficients at the leading order are given as [37]

$$\frac{\partial}{\partial \ln \mu} \mathbf{C} = \mathbf{C} \cdot \mathbf{\Gamma}, \quad (26)$$

where

$$\mathbf{C} = (C_1^q, C_2^q, C_W), \quad \mathbf{\Gamma} = \frac{g_3^2}{16\pi^2} \begin{pmatrix} 8C_F & 0 & 0 \\ 8C_F & 16C_F - 4N_C & 0 \\ 0 & 2N_C & N_C + 2N_f - b_0 \end{pmatrix}. \quad (27)$$

Here, $N_C (= 3)$ and N_f are the number of colors and quark flavors, respectively. $C_F = (N_C^2 - 1)/(2N_C)$ is the Casimir invariant and $b_0 = -11N_C/3 + 2N_f/3$ is the coefficient of the one-loop beta function for g_3 .

B QCD Sum Rules for Nucleon EDMs

In order to get predictions for the nucleon and electron EDMs, we have to estimate the contribution to them from the parton-level interactions. In Ref. [43], the neutron EDM d_n is related to the quark EDMs and CEDMs by using the QCD sum rules at the renormalization scale $\mu = 1$ GeV. Similarly, the proton EDM d_p is also associated with

the quark (C)EDMs at the renormalization scale $\mu = 1$ GeV. The nucleon EDMs are given by using the QCD sum rules as

$$d_N = \frac{-c_0 m_N^3 \langle \bar{q}q \rangle}{\lambda_N^2} \Theta_N, \quad (N = p, n). \quad (28)$$

Here, $c_0 = 0.234$, $\langle \bar{q}q \rangle = -m_\pi^2 f_\pi^2 / (m_u + m_d) = -(0.262 \text{ GeV})^3$ is the quark condensate, and λ_N relates the interpolation fields with the proton and neutron fields. m_N denotes the mass of nucleon N . Θ_N is calculated through the operator product expansions (OPE) for the correlator of interpolation fields and are just the coefficients proportional to $\langle \bar{q}q \rangle$. Without the Peccei-Quinn (PQ) mechanism [50] for the strong CP problem, we obtain

$$\begin{aligned} \Theta_p &= (4e_u m_u \rho_u - e_d m_d \rho_d) \chi \bar{\theta} + (4d_u - d_d) + \left(\kappa - \frac{1}{2} \xi \right) (4e_u \tilde{d}_u - e_d \tilde{d}_d), \\ \Theta_n &= (4e_d m_d \rho_d - e_u m_u \rho_u) \chi \bar{\theta} + (4d_d - d_u) + \left(\kappa - \frac{1}{2} \xi \right) (4e_d \tilde{d}_d - e_u \tilde{d}_u). \end{aligned} \quad (29)$$

Here, e_q , m_q , and d_q (\tilde{d}_q) denote the electric charge for quark q , the mass of quark q , and the (C)EDM for quark q , respectively. χ , κ , and ξ are parameters which relate the quark condensates on the electromagnetic background with $\langle \bar{q}q \rangle$;

$$\begin{aligned} \langle \bar{q} \sigma_{\mu\nu} q \rangle_F &= e_q \chi F_{\mu\nu} \langle \bar{q}q \rangle, \\ g_s \langle \bar{q} G_{\mu\nu}^A T^A q \rangle_F &= e_q \kappa F_{\mu\nu} \langle \bar{q}q \rangle, \\ 2g_s \langle \bar{q} \tilde{G}_{\mu\nu}^A T^A q \rangle_F &= i e_q \xi F_{\mu\nu} \langle \bar{q}q \rangle, \end{aligned} \quad (30)$$

where $\langle \dots \rangle_F$ denotes the vacuum expectation value on the electromagnetic background. These parameters are estimated by Refs. [51, 52], and then the values are given by $\chi = -5.7 \text{ GeV}^{-2}$, $\xi = -0.74$, and $\kappa = -0.34$. ρ_u and ρ_d are defined as

$$\begin{aligned} \rho_u &= \frac{m_*}{m_u} \left\{ 1 + \frac{m_0^2}{2\theta} \left[\frac{\tilde{d}_u - \tilde{d}_d}{m_d} + \frac{\tilde{d}_u - \tilde{d}_s}{m_s} \right] \right\}, \\ \rho_d &= \frac{m_*}{m_d} \left\{ 1 + \frac{m_0^2}{2\theta} \left[\frac{\tilde{d}_d - \tilde{d}_u}{m_u} + \frac{\tilde{d}_d - \tilde{d}_s}{m_s} \right] \right\}. \end{aligned} \quad (31)$$

The parameter m_0^2 which is associated with the VEV of $\bar{q}(G \cdot \sigma)q$ is estimated by Belyaev and Ioffe [51]: $m_0^2 = 0.8 \text{ GeV}^2$. m_* is the reduced quark mass defined as $m_*^{-1} = m_u^{-1} + m_d^{-1} + m_s^{-1}$. The two-loop evolution of λ_N is given as follows:

$$\begin{aligned} \lambda_N(1 \text{ GeV}) &= \left(\frac{\alpha_s(1 \text{ GeV})}{\alpha_s(m_c)} \right)^{-\frac{2}{9}} \left(\frac{\alpha_s(m_c)}{\alpha_s(2 \text{ GeV})} \right)^{-\frac{6}{25}} \\ &\times \left(\frac{\alpha_s(1 \text{ GeV}) + \frac{9\pi}{16}}{\alpha_s(m_c) + \frac{9\pi}{16}} \right)^{\frac{2}{9} - \frac{41}{64}} \left(\frac{\alpha_s(m_c) + \frac{100\pi}{154}}{\alpha_s(2 \text{ GeV}) + \frac{100\pi}{154}} \right)^{\frac{6}{25} - \frac{117}{154}} \lambda_N(2 \text{ GeV}) \\ &= -0.0439 \text{ GeV}^3, \end{aligned} \quad (32)$$

for $\lambda_N(2 \text{ GeV}) = -0.0480 \text{ GeV}^3$. Thus, we obtain the relation between the nucleon EDMs and the quark (C)EDMs as follows:

$$\begin{aligned} d_p &= -1.2 \times 10^{-16} [e \text{ cm}] \bar{\theta} + 0.78d_u - 0.20d_d + e(-0.28\tilde{d}_u + 0.28\tilde{d}_d + 0.021\tilde{d}_s), \\ d_n &= 8.2 \times 10^{-17} [e \text{ cm}] \bar{\theta} - 0.12d_u + 0.78d_d + e(-0.30\tilde{d}_u + 0.30\tilde{d}_d - 0.014\tilde{d}_s). \end{aligned} \quad (33)$$

Even if the PQ mechanism works, the theta parameter is induced as

$$\bar{\theta}_{\text{ind}} = \frac{m_0^2}{2} \sum_q \frac{\tilde{d}_q}{m_q}, \quad (34)$$

and then, we find the OPE coefficients Θ_N as

$$\begin{aligned} \Theta_p &= (4d_u - d_d) + \left(\kappa - \frac{1}{2}\xi + \frac{m_0^2}{2}\chi \right) (4e_u\tilde{d}_u - e_d\tilde{d}_d), \\ \Theta_n &= (4d_d - d_u) + \left(\kappa - \frac{1}{2}\xi + \frac{m_0^2}{2}\chi \right) (4e_d\tilde{d}_d - e_u\tilde{d}_u). \end{aligned} \quad (35)$$

Thus, we find the relation between the nucleon EDMs and the quark (C)EDMs under the PQ symmetry as follows:

$$\begin{aligned} d_p^{\text{PQ}} &= 0.78d_u - 0.20d_d + e(-1.2\tilde{d}_u - 0.15\tilde{d}_d), \\ d_n^{\text{PQ}} &= -0.20d_u + 0.78d_d + e(0.29\tilde{d}_u + 0.59\tilde{d}_d). \end{aligned} \quad (36)$$

References

- [1] ATLAS Collaboration, G. Aad *et al.*, “Observation of a new particle in the search for the Standard Model Higgs boson with the ATLAS detector at the LHC”, *Phys.Lett.* **B716**, 1 (2012), arXiv:1207.7214.
- [2] CMS Collaboration, S. Chatrchyan *et al.*, “Observation of a new boson at a mass of 125 GeV with the CMS experiment at the LHC”, *Phys.Lett.* **B716**, 30 (2012), arXiv:1207.7235.
- [3] ATLAS, CMS, G. Aad *et al.*, “Combined Measurement of the Higgs Boson Mass in pp Collisions at $\sqrt{s} = 7$ and 8 TeV with the ATLAS and CMS Experiments”, *Phys.Rev.Lett.* **114**, 191803 (2015), arXiv:1503.07589.
- [4] S. P. Martin, “Extra vector-like matter and the lightest Higgs scalar boson mass in low-energy supersymmetry”, *Phys.Rev.* **D81**, 035004 (2010), arXiv:0910.2732.
- [5] L. J. Hall, D. Pinner, and J. T. Ruderman, “A Natural SUSY Higgs Near 126 GeV”, *JHEP* **1204**, 131 (2012), arXiv:1112.2703.
- [6] G. F. Giudice and A. Strumia, “Probing High-Scale and Split Supersymmetry with Higgs Mass Measurements”, *Nucl.Phys.* **B858**, 63 (2012), arXiv:1108.6077.
- [7] M. Ibe and T. T. Yanagida, “The Lightest Higgs Boson Mass in Pure Gravity Mediation Model”, *Phys.Lett.* **B709**, 374 (2012), arXiv:1112.2462.
- [8] M. Ibe, S. Matsumoto, and T. T. Yanagida, “Pure Gravity Mediation with $m_{3/2} = 10\text{-}100\text{TeV}$ ”, *Phys.Rev.* **D85**, 095011 (2012), arXiv:1202.2253.
- [9] F. Gabbiani, E. Gabrielli, A. Masiero, and L. Silvestrini, “A Complete analysis of FCNC and CP constraints in general SUSY extensions of the standard model”, *Nucl.Phys.* **B477**, 321 (1996), arXiv:hep-ph/9604387.
- [10] J. Hisano, S. Matsumoto, M. Nagai, O. Saito, and M. Senami, “Non-perturbative effect on thermal relic abundance of dark matter”, *Phys.Lett.* **B646**, 34 (2007), arXiv:hep-ph/0610249.
- [11] W. Altmannshofer, R. Harnik, and J. Zupan, “Low Energy Probes of PeV Scale Sfermions”, *JHEP* **1311**, 202 (2013), arXiv:1308.3653.
- [12] N. Nagata and S. Shirai, “Sfermion Flavor and Proton Decay in High-Scale Supersymmetry”, *JHEP* **1403**, 049 (2014), arXiv:1312.7854.
- [13] M. Tanimoto and K. Yamamoto, “ $K_L \rightarrow \pi^0 \nu \bar{\nu}$ decay correlating with ϵ_K in high-scale SUSY”, *PTEP* **2015**, 053B07 (2015), arXiv:1503.06270.
- [14] J. Hisano, T. Kuwahara, and N. Nagata, “Grand Unification in High-scale Supersymmetry”, *Phys.Lett.* **B723**, 324 (2013), arXiv:1304.0343.

- [15] J. Hisano, D. Kobayashi, T. Kuwahara, and N. Nagata, “Decoupling Can Revive Minimal Supersymmetric SU(5)”, JHEP **1307**, 038 (2013), arXiv:1304.3651.
- [16] G. F. Giudice, M. A. Luty, H. Murayama, and R. Rattazzi, “Gaugino mass without singlets”, JHEP **9812**, 027 (1998), arXiv:hep-ph/9810442.
- [17] L. Randall and R. Sundrum, “Out of this world supersymmetry breaking”, Nucl.Phys. **B557**, 79 (1999), arXiv:hep-th/9810155.
- [18] A. E. Nelson and N. J. Weiner, “Extended anomaly mediation and new physics at 10-TeV”, (2002), arXiv:hep-ph/0210288.
- [19] K. Hsieh and M. A. Luty, “Mixed gauge and anomaly mediation from new physics at 10-TeV”, JHEP **0706**, 062 (2007), arXiv:hep-ph/0604256.
- [20] G. Giudice and A. Masiero, “A Natural Solution to the mu Problem in Supergravity Theories”, Phys.Lett. **B206**, 480 (1988).
- [21] E. Shabalin, “Electric Dipole Moment of Quark in a Gauge Theory with Left-Handed Currents”, Sov.J.Nucl.Phys. **28**, 75 (1978).
- [22] G. Giudice and A. Romanino, “Electric dipole moments in split supersymmetry”, Phys.Lett. **B634**, 307 (2006), arXiv:hep-ph/0510197.
- [23] S. Weinberg, “Larger Higgs Exchange Terms in the Neutron Electric Dipole Moment”, Phys.Rev.Lett. **63**, 2333 (1989).
- [24] J. Hisano and Y. Shimizu, “Hadronic EDMs induced by the strangeness and constraints on supersymmetric CP phases”, Phys.Rev. **D70**, 093001 (2004), arXiv:hep-ph/0406091.
- [25] J. Hisano, M. Nagai, and P. Paradisi, “Flavor effects on the electric dipole moments in supersymmetric theories: A beyond leading order analysis”, Phys.Rev. **D80**, 095014 (2009), arXiv:0812.4283.
- [26] K. Fuyuto, J. Hisano, N. Nagata, and K. Tsumura, “QCD Corrections to Quark (Chromo)Electric Dipole Moments in High-scale Supersymmetry”, JHEP **1312**, 010 (2013), arXiv:1308.6493.
- [27] ACME, J. Baron *et al.*, “Order of Magnitude Smaller Limit on the Electric Dipole Moment of the Electron”, Science **343**, 269 (2014), arXiv:1310.7534.
- [28] C. Baker *et al.*, “An Improved experimental limit on the electric dipole moment of the neutron”, Phys.Rev.Lett. **97**, 131801 (2006), arXiv:hep-ex/0602020.
- [29] W. Griffith *et al.*, “Improved Limit on the Permanent Electric Dipole Moment of Hg-199”, Phys.Rev.Lett. **102**, 101601 (2009).

- [30] J. Hewett *et al.*, “Fundamental Physics at the Intensity Frontier”, (2012), arXiv:1205.2671.
- [31] K. Kumar, Z.-T. Lu, and M. J. Ramsey-Musolf, “Working Group Report: Nucleons, Nuclei, and Atoms”, (2013), arXiv:1312.5416.
- [32] A. Lehrach, B. Lorentz, W. Morse, N. Nikolaev, and F. Rathmann, “Precursor Experiments to Search for Permanent Electric Dipole Moments (EDMs) of Protons and Deuterons at COSY”, (2012), arXiv:1201.5773.
- [33] Storage Ring EDM, Y. K. Semertzidis, “A Storage Ring proton Electric Dipole Moment experiment: most sensitive experiment to CP-violation beyond the Standard Model”, (2011), arXiv:1110.3378.
- [34] W. Dekens *et al.*, “Unraveling models of CP violation through electric dipole moments of light nuclei”, JHEP **07**, 069 (2014), arXiv:1404.6082.
- [35] S. P. Martin, “Generalized messengers of supersymmetry breaking and the sparticle mass spectrum”, Phys.Rev. **D55**, 3177 (1997), arXiv:hep-ph/9608224.
- [36] M. Ciuchini, E. Franco, L. Reina, and L. Silvestrini, “Leading order QCD corrections to $b \rightarrow s\gamma$ and $b \rightarrow sg$ decays in three regularization schemes”, Nucl.Phys. **B421**, 41 (1994), arXiv:hep-ph/9311357.
- [37] G. Degrassi, E. Franco, S. Marchetti, and L. Silvestrini, “QCD corrections to the electric dipole moment of the neutron in the MSSM”, JHEP **0511**, 044 (2005), arXiv:hep-ph/0510137.
- [38] J. F. Kamenik, M. Papucci, and A. Weiler, “Constraining the dipole moments of the top quark”, Phys. Rev. **D85**, 071501 (2012), arXiv:1107.3143, [Erratum: Phys. Rev.D88,no.3,039903(2013)].
- [39] J. Brod, U. Haisch, and J. Zupan, “Constraints on CP-violating Higgs couplings to the third generation”, JHEP **11**, 180 (2013), arXiv:1310.1385.
- [40] F. Sala, “A bound on the charm chromo-EDM and its implications”, JHEP **03**, 061 (2014), arXiv:1312.2589.
- [41] M. Gorbahn and U. Haisch, “Searching for $t \rightarrow c(u)h$ with dipole moments”, JHEP **06**, 033 (2014), arXiv:1404.4873.
- [42] S. M. Barr and A. Zee, “Electric Dipole Moment of the Electron and of the Neutron”, Phys.Rev.Lett. **65**, 21 (1990).
- [43] J. Hisano, J. Y. Lee, N. Nagata, and Y. Shimizu, “Reevaluation of Neutron Electric Dipole Moment with QCD Sum Rules”, Phys.Rev. **D85**, 114044 (2012), arXiv:1204.2653.

- [44] T. Bhattacharya, V. Cirigliano, R. Gupta, H.-W. Lin, and B. Yoon, “Neutron Electric Dipole Moment and Tensor Charges from Lattice QCD”, (2015), arXiv:1506.04196.
- [45] D. A. Demir, M. Pospelov, and A. Ritz, “Hadronic EDMs, the Weinberg operator, and light gluinos”, Phys.Rev. **D67**, 015007 (2003), arXiv:hep-ph/0208257.
- [46] J. Hisano, D. Kobayashi, N. Mori, and E. Senaha, “Effective Interaction of Electroweak-Interacting Dark Matter with Higgs Boson and Its Phenomenology”, Phys.Lett. **B742**, 80 (2015), arXiv:1410.3569.
- [47] J. L. Evans and K. A. Olive, “Universality in Pure Gravity Mediation with Vector Multiplets”, Phys.Rev. **D90**, 115020 (2014), arXiv:1408.5102.
- [48] ATLAS, G. Aad *et al.*, “Search for squarks and gluinos with the ATLAS detector in final states with jets and missing transverse momentum using $\sqrt{s} = 8$ TeV proton–proton collision data”, JHEP **1409**, 176 (2014), arXiv:1405.7875.
- [49] CMS, S. Chatrchyan *et al.*, “Search for new physics in the multijet and missing transverse momentum final state in proton-proton collisions at $\sqrt{s}= 8$ TeV”, JHEP **1406**, 055 (2014), arXiv:1402.4770.
- [50] R. Peccei and H. R. Quinn, “CP Conservation in the Presence of Instantons”, Phys.Rev.Lett. **38**, 1440 (1977).
- [51] V. Belyaev and B. Ioffe, “Determination of Baryon and Baryonic Resonance Masses from QCD Sum Rules. 1. Nonstrange Baryons”, Sov.Phys.JETP **56**, 493 (1982).
- [52] I. I. Kogan and D. Wyler, “A Sum rule calculation of the neutron electric dipole moment from a quark chromoelectric dipole coupling”, Phys.Lett. **B274**, 100 (1992).